DR. STACI MARIE AMBURGEY (Orcid ID : 0000-0002-7100-7811)

DR. NATHAN J. HOSTETTER (Orcid ID : 0000-0001-6075-2157)

DR. BRETT T. MCCLINTOCK (Orcid ID : 0000-0001-6154-4376)

Article type : Articles

Journal: Ecological Applications

Manuscript type: Articles

Running Title: Evaluation of abundance estimators

Evaluation of camera trap-based abundance estimators for unmarked populations

S.M. Amburgey[1,7], A.A. Yackel Adams[2], B. Gardner[3], N.J. Hostetter[1], S.R. Siers[4], B.T. McClintock[5], S.J. Converse[6]

[1] Washington Cooperative Fish and Wildlife Research Unit, School of Aquatic and Fishery Sciences, University of Washington, Seattle, WA, USA 98195

[2] U.S. Geological Survey, Fort Collins Science Center, 2150 Centre Avenue, Building C, Fort Collins, CO, USA 80526

[3] School of Environmental and Forest Sciences, University of Washington, Seattle, WA, USA 98195

[4] U.S. Department of Agriculture APHIS Wildlife Services National Wildlife Research Center, 233 Pangelinan Way, Barrigada, GU 96913

[5] Marine Mammal Laboratory, NOAA-NMFS Alaska Fisheries Science Center, Seattle, WA, USA 98115

[6] U.S. Geological Survey, Washington Cooperative Fish and Wildlife Research Unit, School of Environmental and Forest Sciences & School of Aquatic and Fishery Sciences, University of Washington, Seattle, WA, USA 98195

[7] Corresponding author. E-mail: staci.m.amburgey@gmail.com

Manuscript received 1 September 2020; revised 5 January 2021; accepted 3 March 2021; final version received 9 July 2021.

Abstract:

Estimates of species abundance are critical to understand population processes and to assess and select management actions. However, capturing and marking individuals for abundance estimation, while providing robust information, can be economically and logistically prohibitive, particularly for species with cryptic behavior. Camera traps can be used to collect data at temporal and spatial scales necessary for estimating abundance, but the use of camera traps comes with limitations when target species are not uniquely identifiable (i.e., “unmarked”). Abundance estimation is particularly useful in the management of invasive species, with herpetofauna being recognized as some of the most pervasive and detrimental invasive vertebrate species. However, the use of camera traps for these taxa presents additional challenges with relevancy across multiple taxa. It is often necessary to use lures to attract animals in order to obtain sufficient observations, yet lure-attraction can influence species’ landscape use and potentially induce bias in abundance estimators. We investigated these challenges and assessed the feasibility of obtaining reliable abundance estimates using camera trapping data on a population of invasive brown treesnakes (*Boiga irregularis*) in Guam. Data were collected using camera traps in an enclosed area where snakes were subject to high-intensity capture-recapture effort, resulting in presumed abundance of 116 snakes (density = 23/ha). We then applied Spatial Count, Random Encounter and Staying Time, Space to Event, and Instantaneous Sampling estimators to photo-capture data to estimate abundance and compared estimates to our presumed abundance. We found that all estimators for unmarked populations performed poorly, with inaccurate or imprecise abundance estimates that limit their usefulness for management in this system. We further investigated the sensitivity of these estimators to the use of lures (i.e., violating the assumption that animal behavior is unchanged by sampling) and camera density in in a simulation study. Increasing the effective distances of a lure (i.e., "lure attraction") and camera density both resulted in biased abundance estimates. Each estimator rarely recovered truth or suffered from convergence issues. Our results indicate that, when limited to unmarked estimators and the use of lures, camera traps alone are unlikely to produce abundance estimates with utility for brown treesnake management.

Keywords: bait attraction, brown treesnakes, *Boiga irregularis*, density, Guam, invasive species, random encounter and staying time, sampling design, simulation, spatial capture-recapture, space to event

Introduction

Abundance estimation is central to wildlife ecology and management. For example, abundance estimation contributes to management decisions through the listing and active management of species experiencing population declines (IUCN 2001, Reynolds et al. 2011), the assessment of hunter-harvest success (Nichols et al. 2007, Mitchell et al. 2018), the determination of species reintroduction success (Armstrong and Seddon 2008, Jachowski et al. 2016), and the evaluation of suppression or eradication efforts for invasive species (Ramsey et al. 2009, Link et al. 2018). However, reliable abundance estimation remains challenging to accomplish. The collection of data necessary for abundance estimation (e.g., capture-recapture) can be labor and cost intensive (Pollock et al. 2002), especially for species that are rare or display cryptic behavior. Abundance indices (e.g., scat counts, aerial survey counts; Tracey et al. 2005, Brodie 2006) may be more affordable to obtain but often do not account for sources of nondetection bias nor include estimates of uncertainty, limiting their use in management decisions (Williams and Thomas 2009, Converse et al. 2013). The need for precise abundance estimates has spurred technological advances in wildlife monitoring to reduce tradeoffs between data collection gains and financial and logistical costs (Karanth and Nichols 1998, Waits and Paetkau 2005, Bohmann et al. 2014).

Out of these monitoring technologies, camera trapping has emerged as one of the most well-known and widely used sampling protocols for terrestrial species with cryptic behavior in the last several decades (O’Connell et al. 2011, Royle and Gardner 2011, Rovero and Zimmermann 2016, Gilbert et al. 2020). Game or trail cameras (henceforth, camera traps) can be programmed to automatically sample on a specified schedule and placed unobtrusively across the landscape, requiring only infrequent maintenance and thus reducing the amount of fieldwork necessary to collect data over large spatial extents (Karanth and Nichols 1998, O’Connell et al. 2011). Processing these photos, whether manually or via automated processes (e.g., machine learing; Norouzzadeh et al. 2018), results in a series of species detections at each camera over time. Unique markings (e.g., pelage patterns) can be used to identify individuals, and estimates of abundance can thereby be obtained through a capture-recapture or spatial capture-recapture (SCR) analysis framework (Karanth and Nichols 1998, Royle and Gardner 2011, Royle et al. 2014). However, individual identification in photographs is not possible for many species. There are abundance estimators based solely on encounter data from unmarked individuals (i.e., unmarked estimators; e.g., Royle 2004, Rowcliffe et al. 2008, Chandler and Royle 2013, Moeller et al. 2018, Nakashima et al. 2018). These estimators have assumptions about how animals move and are detected, which may require additional knowledge about species life history, movement ecology, or sampling design and equipment (Table 1; Chandler and Royle 2013, Dénes et al. 2015, Moeller et al. 2018, Gilbert et al. 2020).

Estimation of species abundance is integral to invasive species management as it can indicate predation or competition risk to native species, offer a measure of removal success, and provide guidance for prioritization of management efforts (Maguire 2004). The management of invasive species is of pressing global importance in order to minimize loss of native biodiversity, ecosystem services, and tourism revenue (Mooney and Hobbs 2000, Rodda and Savidge 2007, Kraus 2009, Pejchar and Mooney 2010). Yet the cost of monitoring and managing established invasive wildlife can be prohibitive (Pimentel et al. 2005, Larson et al. 2011). Managers require effective monitoring tools at an acceptable cost tradeoff, and these tools must be able to provide sufficient data to reliably estimate target parameters in order to inform management decisions. Camera trapping provides a means to minimize monitoring costs, but certain invasive species, such as herpetofauna (i.e., amphibians and reptiles), can complicate the use of cameras in both familiar and novel ways.

Reptiles and amphibians are some of the most ecologically and economically damaging invasive vertebrates (Kraus 2009, 2015). Their suppression and eradication is complicated by the fact that they are frequently behaviorally cryptic, slow-moving, and prone to engage in long periods of inactivity (e.g., post-meal consumption; Siers et al. 2018). Monitoring is complicated by the frequent lack of uniquely identifiable marks, thus requiring physical capturing and marking. This slow-moving and cryptic lifestyle of herpetofauna specifically presents a challenge for camera trapping as the likelihood of the target species encountering and triggering a camera trap may be low. Detection of herpetofauna on camera traps is also complicated by the lack of locations such as game trails that would ensure well-traveled or predictable pathways for movement and increase the likelihood of detecting animals as they move around the landscape (Cusack et al. 2015). Using traps with bait or lures can increase the likelihood of an animal encountering a trap and being sampled, but this may violate abundance estimator assumptions concerning habitat use (e.g., Moeller et al. 2018, Nakashima et al. 2018). Additionally, these ectothermic, slow-moving, generally small species often are not detected on commonly used passive infrared (PIR) cameras that rely on motion and thermal signatures to trigger a photograph (e.g., Reconyx Inc. 2013). Channeling animal movement to break a near infrared beam is useful for sampling some species (Hobbs and Brehme 2017), though not possible for all species (e.g., arboreal species) and thus sampling frequently requires the automated time-lapse feature to be used on cameras (Yackel Adams et al. 2019). Depending on the selected time interval between photographs and the length of the study, this results in thousands or millions of photographs to process. Despite these challenges, camera trapping may still be useful for monitoring herpetofauna when alternative sampling methods are prohibitively expensive. Focusing on invasive brown treesnakes (*Boiga irregularis*), we assess whether sufficient camera trap data can be collected to obtain reliable population abundance estimates for a species with cryptic behavior that requires the use of lures to obtain an adequate sample of detections on cameras.

Brown treesnakes are an ecologically and economically detrimental invasive species now prevalent across the U.S. territory of Guam, the southernmost island in the Mariana Islands (Fig. 1). They are nocturnal, arboreal, and generalist predators (Rodda and Savidge 2007). Their accidental introduction in the 1940s and subsequent invasion resulted in the decimation of the local avifauna and declines in other native vertebrate populations (Savidge 1987, Fritts 1988, Rodda et al. 1992, Rodda and Savidge 2007). The ability to track changes in brown treesnake abundance is particularly important for evaluating the effectiveness of management techniques, such as a novel system for automated aerial delivery of toxic baits for landscape-scale suppression (Siers et al. 2020). Monitoring to obtain abundance estimates of brown treesnakes is also important in the conservation of remaining native species and the potential reintroduction of those that have been locally extirpated. Economic and ecological risks are high when considering the reintroduction of endangered species on Guam as a single brown treesnake is capable of eating (or biting and killing without consuming) several prey items in a single evening (Savidge 1987, Lardner et al. 2009, J.A. Savidge *pers. comm.*). Precision in abundance estimates is therefore crucial to the management of this system. Abundance estimation can be achieved through the marking and recapture of individuals. However, as brown treesnakes are behaviorally cryptic, arboreal, and live in complex habitat, detection probability during a survey is low (when done at comparable levels of sampling intensity; $\hat{p} = 0.07$ for visual surveys, Christy et al. 2010 and $\hat{p} = 0.14$ for trapping, Tyrrell et al. 2009).

We investigated the potential utility of time-lapse camera traps for estimating snake abundance. These camera traps were set to view snake traps containing a live mouse lure in a protected chamber that attract but potentially do not always capture snakes. We conducted this work in a fenced (i.e., geographically closed), intensively monitored population of brown treesnakes on Guam for which we obtained a precise abundance estimate (hereafter referred to as the “presumed abundance”) based on SCR methods. This provided a unique opportunity to validate the use of camera trapping for abundance estimation. Field evaluation is an important yet rarely accomplished process that allows for real-world comparisons of methodologies

(Gilbert et al. 2020). We used four common estimators for unmarked populations that were applicable to our study system: Spatial Count (SC; Chandler and Royle 2013); Random Encounter and Staying Time (REST; Nakashima et al. 2018); and Space To Event and Instantaneous Sampling (STE and IS; Moeller et al. 2018). Additionally, we conducted a simulation study to investigate: 1) the degree to which the use of lures may violate the assumptions of these estimators and the impact that has on abundance estimates; and 2) whether increasing the density of camera traps could improve abundance estimation. We present an assessment of the feasibility of using camera traps in an invasive population given the need for reliable abundance estimates for management.

Materials and Methods

Field Sampling

Data collection for this study was conducted by U.S. Geological Survey (USGS) biologists within a 5-hectare (50,000 m^2) fenced section of forest located on Andersen Air Force Base (AAFB) on Guam (Fig. 1 and 2A). This area, known as the Closed Population (CP), was constructed in 2004 with the goal of creating a population of presumed abundance and thoroughly-studied demography of brown treesnakes in the field to assess the efficacy of monitoring and control tools in addition to tracking changes over time and in response to management actions (e.g., Tyrrell et al. 2009, Christy et al. 2010, Lardner et al. 2013, Nafus et al. 2018, Siers et al. 2018). The CP was surrounded by a two-way barrier fence (Fig. 2B; Perry et al. 1998, Rodda et al. 2007) composed of a 1.5 m high chain link fence covered on both sides with a welded-wire galvanized mesh (6.3 mm square wire spacing) and bounded by a 0.5 m concrete footer with vegetation removed from 2 m to either side of the fence. The wire mesh was also formed into a protruding bulge on both sides, at approximately 1.2 m above ground level, preventing snakes from maintaining traction while climbing and effectively eliminating immigration into or emigration out of the area.

In 2015, a camera trapping study was conducted in the CP. Eight camera traps (Reconyx Hyperfire model, Reconyx, Holmen, WI) were placed along a series of permanent, parallel transects lined with pre-established georeferenced grid markers that span the entirety of the CP, comprising a 13 × 13 grid of markers with approximately 16-m spacing (Fig. 2A). Cameras were rotated through six different transect and grid marker locations (48 total camera trap locations), with each camera in place for seven or ten days (Appendix S1: Table S1). In a given evening, all 13 grid markers (with and without cameras) along an "active" (i.e., surveyed) transect had dual-funnel snake traps equipped with one-way entrance flaps containing live mice as lures, with mice protected from consumption in separate cages within the snake traps (Fig. 2C; Rodda et al. 1999a). Reconyx cameras were custom-focused to 1.83 m, the distance in front of cameras where mouse-lure traps were placed. Mouse-lure traps were checked daily and trapped snakes were released back into the CP (only 5 snakes were captured at traps with cameras during the entire study). Using the time-lapse feature, camera traps were programmed to take photos every 30 seconds from 6pm to 6am (the documented activity period for brown treesnakes; Rodda et al. 1999b, Siers et al. 2018) for 45 days (27 February-13 April 2015).

Photo processing was performed manually, with USGS biologists checking all photos and recording when a snake entered the field of view (FOV), exited the FOV, and behavior of the animal when present. Several unmarked estimators used in this paper assume perfect detection of the target species within a specified area of the camera (requiring a known depth of FOV; Table 1). To ensure this assumption was met, photos were further processed to retain only detections of snakes up to 1.83 m from the camera, i.e., only records of snakes that were on or in front of the mouse-lure trap were retained for analyses.

Obtaining the Presumed Abundance

Over the course of several studies, extensive visual, hand-capture, and trapping surveys were conducted intermittently along the parallel transects in the CP, starting in 2004 and continuing through 2015. Surveys were done multiple times within a week and during multiple weeks within a month. Biologists caught, measured, and marked snakes (through passive integrated transponder tags and unique, ventral scale clipping patterns not visible without the handling of animals). We determined the likely abundance of snakes in the CP using these data from 2013 and 2015-2018 (capture-recapture studies were not conducted during 2014). For abundance comparisons, we used the number of marked snakes in the size (snout-vent length) range that could be attracted to mouse-lure traps and thus the proportion of the population that would be detectable on cameras (i.e., snakes ≥700 mm; Rodda et al. 2007, Tyrrell et al. 2009, Yackel Adams et al. 2019). Brown treesnakes have size-structured prey-preferences, where smaller snakes (<700 mm) largely avoid mammalian prey, partly due to being gape-limited (Savidge 1988) and partly due to a preference for lizard prey (Lardner et al. 2009).

We counted all animals caught in 2015 (n = 111 snakes). We also checked for individuals caught in 2013 and again in 2016, 2017, or 2018, implying they were alive during the 2015 sample period. However, no snakes caught in 2013 and observed in 2016 or later were not also observed in 2015. Newly captured snakes in the CP are often smaller individuals that are born inside the study area and eventually grow to a size that is more detectable during visual searches or trappable using mouse-lures. Therefore, n = 5 brown treesnakes that were newly marked in 2016 at ≥900 mm in size, and were therefore likely ≥700 mm during 2015 but not captured, were included, resulting in a presumed abundance of 116 (111 + 5) brown treesnakes of trappable size in 2015.

We also performed a spatial capture-recapture analysis (Royle et al. 2013; Data S1) on data collected in the CP during the same period of time as the 2015 camera trapping study, using captures of animals ≥700 mm. This analysis allowed us to assess our presumed snake abundance in addition to providing parameter estimates for use as informed priors in the SC estimator. These extensive survey data and verification via spatial capture-recapture estimation allowed for the rare situation in which abundance estimates obtained from unmarked estimators can be compared to a population with a highly accurate and precise abundance estimate.

Data Analysis

We used four estimators to estimate abundance and density from the CP camera trap data. For consistency across estimators, each of the j = 1, 2, …, J camera trap locations are denoted by $\boldsymbol{x}_j$ within the CP study area, S, also called the state-space in SCR terminology. As trap locations were originally established using a standardized grid, camera locations were identified by grid cell. The total area of the CP (A) was 50,000m^2. Surveys occurred on k = 1, 2, …, K occasions, but the length of an occasion varied by estimator. Across all estimators, abundance and density are denoted by N and D, respectively. Density was calculated as $D = N/A$ (note that the state-space area, S, was equal to A) unless otherwise noted. We calculated the camera FOV area, a, as an equilateral triangle with depth 1.83m (a = 1.93m^2). We assumed perfect detection in the FOV for this study. Each estimator is described below with additional details of estimators in the primary literature (Chandler and Royle 2013, Moeller et al., 2018, Nakashima et al. 2018), and analysis code available in Data S2. We use the originally published notation for each estimator (based on the code appendices), meaning that the symbols used for parameters may change meaning depending on the estimator being discussed but are denoted by subscripts.

Spatial Count

Spatial count (SC) models for unmarked populations rely on spatial auto-correlation in species detections at trapping locations to estimate the number of animals within a study area. Following Chandler and Royle (2013), the counts of animals at each trap j across the entire study period ($n_{j.}$) are assumed to be Poisson-distributed random variables, where

$$n_{j.} \sim Poisson(\Lambda_{j,SC.} K_j).$$

Here, K_j is the number of days a camera trap was active and $\Lambda_{j,SC.}$ denotes the expected encounter rate at trap j per occasion (day) across all individuals. K_j allows for variation in survey effort across the study period (e.g., traps rotating around grid marker locations). To calculate $n_{j.}$, we defined rules for unique snake encounters. Brown treesnakes frequently stay for a period of time in the vicinity of a trap when a mouse-lure is present, entering and exiting the FOV several times. In order to avoid non-independent encounters of the same individual, we defined unique events as animals that were not in the FOV within 30 minutes of each other, or animals that were present in the FOV at the same time and so were known to be unique individuals.

The trap-specific encounter rate $\Lambda_{j,SC.}$ is a function of the latent population size in the state space (N), the distance between an individual activity center and trap j, and two encounter rate parameters: one describing the baseline expected encounter rate at a distance of zero ($\lambda_{0,SC}$) and one describing the decline in expected encounter rates as distance between traps and activity centers increases (σ). We used a data augmentation approach fit in a Bayesian framework to model these processes (Chandler and Royle 2013). Here, latent indicator variables z_i denote whether individual i was part of the population (1) or not part of the population (0). We assume $z_i \sim$ Bernoulli(ψ), for i = 1, 2, …, M individuals where M is set at a value much greater than the expected abundance (Chandler and Royle 2013). The latent activity center of individual i ($\boldsymbol{s}_i$) denotes the coordinates of individual i's average location and informs the expected rate of encounters at trap j ($\lambda_{ij,\ SC}$). We assumed a half-normal detection function for encounter rates. Specifically,

$$\lambda_{ij,\,SC} = \lambda_{0,SC} e^{\left(\frac{-\|\boldsymbol{s}_i - \boldsymbol{x}_j\|^2}{2\sigma^2}\right)} z_i$$

where the numerator is the squared Euclidean distance between each $\boldsymbol{s}_i$ and $\boldsymbol{x}_j$. Note that the latent indicator variable z_i prevents encounters of individuals that are not part of the population. The expected total encounter rate at trap j across all individuals is then derived as $\Lambda_{j.,SC} = \sum_{i=1}^{M} \lambda_{ij,SC}$. Abundance is derived as $N = \sum_{i=1}^{M} z_i$.

We initially used vague priors where $s_i \sim Uniform[S]$, $\lambda_{0,SC} \sim Uniform(0, 5)$, $\psi \sim Uniform(0, 1)$, and $\sigma \sim Uniform(0, 50)$. However, to investigate whether knowledge of snake movement ecology could help improve abundance estimation, we also fit a model with an informed prior such that $\sigma \sim Gamma(274.69, 7.27)$ based on the posterior distribution of σ (i.e., using the mean and standard deviation) from the SCR analysis on hand-captured and trapped individuals (Appendix S2). We also evaluated a scale prior for abundance where $\psi \sim Beta(1e^{-6}, 1)$ (Link 2013, Gerber and Parmenter 2015). This resulted in four parameterizations: vague σ and ψ, informed σ and vague ψ, vague σ and informed ψ, and informed σ and ψ (Table 2). We found that augmentation to M = 500 was adequate to contain the full posterior distribution of abundance for most of our parameterizations, though M = 1000 was needed when we used vague priors for σ and ψ.

Random Encounter and Staying Time

The Random Encounter and Staying Time (REST) model uses the number of encounters and amount of time an animal was present in front of a camera trap (i.e., staying time) to estimate density (Nakashima et al. 2018). Staying time is inversely proportional to animal movement speed and is readily obtainable from camera trapping data. Staying time can be measured through motion-triggered cameras that record video or, as in our study, by multiplying the number of frames containing an individual by the time-lapse interval between photographs to get staying time in seconds. As the REST model has no extension for imperfect detection within the camera FOV area, we caution that a time-lapse interval must be shorter than the minimum time it would take an animal to enter and exit the FOV, so that individuals are not missed and that staying time is properly reflected.

The data required for the REST model include trap-specific FOV area (a_j), trap-specific effort (ξ_j; i.e., length of time camera j was operational multiplied by the activity proportion), total encounters per trap (y_j), and staying time (x_i) for each of the $i = 1,2,...,\sum_j y_j$ encounters. The activity proportion corrects for the proportion of individuals that are active and available for detection during sampling. The REST model relies on the concept that the number of encounters at trap j is a function of FOV area (a_j), effort (ξ_j), density (D), and mean staying time (${\lambda^{-1}}_{REST}$). Following Nakashima et al. (2018), we assume the number of encounters at camera trap j, y_j, is a Poisson random variable with mean rate μ_j, $\quad y_j \sim \text{Poisson}(\mu_j)$.

The staying times for each individual encounter (x_i) are modeled as exponentially distributed random values with mean ${\lambda^{-1}}_{REST}$, or $x_i \sim \text{Exp}(\lambda_{REST})$. The mean rate of encounters at camera j (μ_j) is itself a function of density (D), FOV area (a_j), trap specific effort (ξ_j), and mean staying time (${\lambda^{-1}}_{REST}$) where

$$\mu_j = D a_j \xi_j {\lambda^{-1}}_{REST}.$$

In the REST model, D is directly estimable because a_j and ξ_j are provided as data, ${\lambda^{-1}}_{REST}$ is estimated from individual staying time, and μ_j is estimated from trap-specific encounters. Abundance is then derived as $N = D \times A$.

In our study, staying time (x_i) was the sum of time (in seconds) that an individual remained present across consecutive time-lapse photographs. The REST model also allows for the censoring of staying times that stretch beyond the period in which cameras are operational. We censored the staying time of one snake that stayed in the FOV for an entire evening as this behavior, while not unusual for snakes hiding and digesting large meals (Siers et al. 2018), was not representative of snakes that are active, and therefore was excluded because activity proportion is accounted for in the model.

We used vague priors where $\lambda_{REST} \sim Uniform(0,5)$ and $D \sim Gamma(0.1,0.1)$. We assumed *a priori* that brown treesnake activity might be around 0.6 based on previous work concerning the duration of active foraging vs. digestion cycles (Siers et al. 2018). However, given our presumed abundance, we were able to calculate ξ_j using different activity proportions (0.2, 0.4, 0.6, 0.8, 1.0) to see what value would return the closest estimate to N = 116 snakes. We ran five models where we calculated sampling effort as the product of 12 hours of camera trapping (43,200 seconds per day) over 45 days of sampling and these different activity proportions.

Space to Event

The space to event (STE) model (Moeller et al. 2018) uses the area searched (i.e., camera FOVs) until an encounter occurs to estimate the abundance and density of individuals within a target area. The STE model relies on the camera time-lapse function so that sampling data can be defined as the simultaneous and instantaneous animal observations at all camera traps at specified times (i.e., the animals present in each FOV at the same sampling time). The order in which camera FOVs are searched is randomized at each time. Perfect detection is assumed within the camera FOV. This shifts the estimation of abundance from relying on the rate at which individuals encounter camera traps to how much space was searched before an animal was detected during a given sample. For example, if on occasion k = 5 we detected an animal at the third camera, this would result in a space to event of $R_{k=5} = \sum_{j=1}^{3} a_j$ where a_j is the FOV area for camera j. If no animal was observed on a camera during an entire occasion, then the space needed to detect an animal was greater than all our camera FOVs, and data are right censored.

Space to event data on occasion k, R_k, are modeled as exponential random variables such that $R_k \sim Exp(\lambda_{STE})$, where λ_{STE} is the rate parameter describing the expected number of individuals per unit of space. Abundance can then be estimated as $N = \lambda_{STE} * A$. We used a vague prior for the rate parameter, $\lambda_{STE} \sim Uniform(0{,}5)$. In order to ensure independent samples at cameras, we determined thirty-minute intervals would, on average, prevent the same individual from being repeatedly detected at the same camera. That resulted in 25 sampling occasions within a day (from the start of cameras at time 0 to the 12-hour mark) for each of the 45 days.

Instantaneous Sampling

The Instantaneous Sampling (IS) estimator (Moeller et al. 2018) is a simplified estimator for the abundance of unmarked populations, scaling from the total count of animals observed in the total area sampled via camera traps to the abundance of animals in the overall study area. This uses the same data required as the STE model but instead uses the count of all encounters observed at a camera and occasion (n_{jk}) across all FOVs at simultaneous and instantaneous samples to estimate abundance and density. Abundance can be estimated with a closed-form expression as

$$N = \frac{1}{K} \cdot \frac{1}{J} \sum_{j=1}^{J} \sum_{k=1}^{K} \frac{A}{a_{jk}} n_{jk}$$

while confidence intervals (CIs) are obtained via bootstrapping. We used 100 resamples for bootstrapping.

Implementation

The first three estimators were fit in a Bayesian framework in JAGS (Plummer 2003) via the jagsUI package (Kellner 2018) in R (R Core Team 2019; Data S2). We ran all models using three chains comprised of 40,000 iterations with 10,000 iterations discarded after burn-in and thinned by 20 to reduce the size of stored files. Model convergence was determined by visual inspection of traceplots and Gelman Rubin statistics ($\hat{R} \leq 1.1$; Gelman et al. 2013). The IS estimator was also implemented and bootstrapping was carried out in R.

Simulation Study

We used computer simulation to determine: 1) if lure attractants can induce bias in the four abundance estimation approaches; and 2) if increasing camera densities could improve estimator performance. We aimed to simulate our study system of brown treesnakes to investigate robustness of the abundance estimators as we changed lure attraction and trap density. We avoided using our estimation models to simulate the data as we would expect the generating model to perform best. Instead, we developed a neutral way in which to simulate data for comparison between estimators.

We simulated movement data of 120 snakes in a similar landscape (~5-ha study area closed to immigration and emigration) during a similar sampling period (12 hours of sampling/day over 45 days). To investigate if and to what degree the effective distance of a lure (henceforth, "lure attraction") could influence estimates, we simulated three levels of attraction: 1) no attraction (i.e., snake movement was uninfluenced by the placement of traps), 2) low attraction (i.e., snake movement could be influenced by mice-lures but only within a buffer of 5-m around a trap), and 3) high attraction (i.e., snake movement could be influenced by mice within a 20-m circumference; A. Yackel-Adams, *pers. comm.*). We simulated cameras in 5 different orientations: 1) the original sampling design used in 2015 (i.e., 8 cameras rotated among 48 different locations on the same schedule; Video S1), 2) a static design (i.e., 8 cameras simulated randomly with no rotation), 3) a static design with double the cameras (i.e., 16 cameras simulated randomly with no rotation), 4) a static design with triple the cameras (i.e., 24 cameras simulated randomly with no rotation), and 5) a static design with six times the cameras (i.e., 48 cameras simulated randomly with no rotation). Based on the estimate of σ from the SCR estimator, 24 cameras at least 16 m apart (due to spacing on the sampling grid) would result in approximately two cameras per area of individual use (aka, home range in territorial species), which fits with recommended camera densities (Rovero et al. 2013, Zimmermann et al. 2013). However, we also tried a scenario with 48 cameras (9.6 cameras/ha) to maximize the density and spatial coverage of our traps on the landscape. This resulted in 15 different survey designs in which snake movements were simulated 100 times each, which we ran using the R package momentuHMM (McClintock and Michelot 2018). Using potential functions (e.g., Brillinger et al. 2012), we simulated snake movement in discrete time using a bivariate normal correlated random walk with bias attributable to covariates that influence the direction of snake movement. Covariates included the study area boundary (to indicate when snakes approached a boundary and should be turned away) and mouse-lure traps (to indicate when snakes approached a trap and should be turned towards it; Fig. 3). Snake movement was simulated every hour in order to minimize computational time while maintaining the information necessary to process data for subsequent analysis. We specified the mean and standard deviation of step length per hour based on Siers et al. (2014), where snakes were located via telemetry every day after the snakes moved overnight (approximately 6pm to 6am) and resettled. We divided the mean daily relocation distance by 12 hours to obtain a rough estimate of hourly snake step length for our simulations.

The output from momentuHMM is a dataset of snake identities and hourly locations within the study area. We calculated the geometry of all snake movement paths and overlaid these paths with camera FOVs. By intersecting these pathways and the camera FOVs, we were able to generate a dataset of when and where snakes would be detected on a camera (Fig. 3). We then processed the data according to the requirements of each analytical approach. For example, for the SC model, we previously defined a unique snake detection event as when snakes within the FOV were at least 30 minutes apart or occurred in the FOV at the same time. By calculating the length of snake pathways into, within, and outside of the FOV, we were able to sum the time between snakes within the FOV in addition to snakes that directly overlapped in time to eliminate non-unique detections. Additionally, the REST model requires the staying time of each animal within a FOV. Given that snakes moved at a constant speed during the simulation, this was obtainable by calculating the proportion of the hour-long path of a snake that was spent within the FOV. Lastly, the STE and IS models rely on instantaneous and synchronized sampling of all cameras at designated times, which we defined as occurring every thirty minutes. Similar to the staying time calculation, this was obtainable by calculating an entry and exit time to the FOV based on where the snake path intersected the FOV. Each dataset was then analyzed using the same estimators detailed above and the code found in Data S2. SC models were analyzed using vague priors and $M = 500$. We subsequently assessed estimator performance by calculating 1) percent relative bias (PRB; the mean difference between estimated mean and true abundance as scaled by true abundance * 100), 2) percent coefficient of variation (CV; the mean of each simulation's standard deviation of the posterior distribution of abundance divided by the estimated mean abundance * 100), 3) nominal coverage (Coverage; the percentage of simulations where 95% highest posterior density interval [HDPI] or CI overlapped true snake abundance), and 4) when applicable, percent model convergence (Convergence; the percentage of simulations of the total converged where $\hat{R} < 1.1$ for each lure attraction-camera density scenario). Although rarely reported, the adequacy of model convergence is of particular interest to our study and serves as a metric to compare the ability of each sampling scenario to collect sufficient data for each estimator and also to assess the performance of each estimator across all simulations. If convergence for all parameters was not achieved, estimates from that simulation were not used to calculate 1-3 above.

Results

Case study

Over the 45-day sampling period, each camera generated 64,800 photographs (total = 518,400). We retained 197 photo-captures for analysis. As each approach relied on specific rules to define unique observations and sampling occasions, the total observations used for each estimator differed (SCR unmarked = 183, REST = 197, STE and IS = 110). Based on extensive (primarily hand) captures of this closed population, we estimated the abundance in 2015 to be 116 snakes that were of a size to be sampled by camera traps with mouse-lures (*D* = 23/ha). Results from the SCR marked estimator support this value, with a mean estimate of 124.35 snakes (HDPI = 110, 140; Appendix S2). As this supports our original estimate, we treated 116 snakes as the presumed abundance for comparison with unmarked estimator results.

Estimates of snake abundance, density, and their associated precision varied by estimator (Table 2; Fig. 3), with estimates from SC models producing particularly long upper tails and thus resulting in modes of abundance that differ markedly from mean abundance (note: we present mean abundance estimates within text). Abundance estimates from SC models varied based on whether vague or informed priors were used (Table 2). The model with vague priors only fully explored the posterior space when using $M = 1000$, estimating 167.83 snakes (HDPI = 9, 546; $D = 34$/ha). All other SC parameterizations showed adequate mixing and searching at $M = 500$. When using an informed prior on σ from the SCR analysis, abundance estimates were much lower than the presumed abundance, with an estimated 10.11 snakes (HDPI = 4, 18; $D = 2$/ha). When using this same informed prior on σ and $\psi \sim Beta(1e^{-6}, 1)$, the estimated number of snakes was similarly low (8.61 snakes, HDPI = 4, 15). Out of the SC estimator parameterizations we tried, snake abundance was closest to the presumed abundance when we used a vague prior on σ and modeled $\psi \sim Beta(1e^{-6}, 1)$. However, with an estimated abundance of 74.23 snakes (HDPI = 7, 174; $D = 15$/ha), this value was more than one and a half times less than presumed abundance. We caution that traceplots for this model also showed mild autocorrelation though $\hat{R} < 1.05$, which was true for nearly all SC models.

For the REST model, estimates of snake abundance varied widely by the activity proportion used but HDPI never contained truth. Estimates ranged from 1061.52 snakes (HDPI = 863, 1275; $D = 212$/ha) when assuming 20% of snakes were active to 212.64 snakes (HDPI = 172, 256; $D = 43$/ha) when assuming 100% of snakes were active during sampling. Our *a priori* assumption of 0.6 as a reasonable approximation of the activity proportion of brown treesnakes produced an estimate of 352.80 (HDPI = 287, 425; D = 71/ha) snakes. All REST models had $\hat{R}$ < 1.05 and adequate mixing of chains indicating convergence.

For the STE model and IS estimator, abundance estimates were not close to the presumed abundance and intervals also never contained truth, with 191.65 (HDPI = 152, 238; D = 38/ha) and 213.63 (95% CI = 172.4, 258.6; D = 43/ha) snakes estimated respectively. Similarly, the STE model diagnostics indicated model convergence.

Simulation

Using the same rules as our case study to process data, we retained a different number of simulated observations per estimator. In all instances the number of snakes that passed through the FOVs increased with increasing lure attraction and simulated camera density, and we present numbers of observations for the REST estimator as a representative example (note: the other estimators retained fewer observations due to more stringent rules for unique capture events). When using no lure, we obtained, on average, 64.1 observations using 8 static cameras and 453.16 observations using 48 static cameras. When using 8 static cameras, we obtained, on average, 64.4 observations with no lures as compared to 2539.9 observations with high-attraction lures. Rotating cameras picked up more observations without and with the use of lures (80.3 with no lures and 5250.72 with high attraction lures) as snakes were able to follow the camera to new areas and moving cameras intersected with more individual areas of use (Video S1). Additionally, moving cameras meant that more observations fit the criteria for being far enough apart in time to be considered unique events for the SC estimator.

Estimator Peformance

Spatial Count

Mean abundance estimates ranged from 43.67 to 271.01 snakes (Table 3; Fig. 4). On average, high-lure attraction scenarios had 1.13 times the number of snakes of no-lure scenarios at the same camera densities. Increasing camera density did not improve abundance estimates, with snake abundance never stabilizing but generally increasing with additional cameras on the landscape (Table 3). Percent relative bias was negative when using only 8 static cameras but increased and became positive at higher camera densities and with rotating camera locations (Table 3). Higher lure attraction scenarios also generally showed greater PRB.

Compared to all other estimators, CV was highest for the SC estimator. The CV decreased on average 34.8% from no to high lure attraction at the same camera density (Table 3). Coverage varied by scenario, where 8 static cameras had low coverage (12-52%, with decreasing coverage as lure attraction increased) while the remainder of scenarios had 38-86% coverage (with no consistent relationship to lure attraction; Table 3). Convergence varied across scenarios, ranging from 82-100% for most scenarios (Table 3) though scenarios with 48 cameras had some of the lowest rates of convergence (63-93%). There was a general trend of reduced convergence at higher lure attraction and camera densities. The scenario using 16 static cameras at low levels of lure attraction had the closest estimate to truth (126.20 snakes with PRB = 5.16), though CV was relatively high (61.78%), HDPI contained truth in only 73% of the simulations, and convergence was achieved in only 86% of simulations.

Random Encounter and Staying Time

Mean abundance estimates ranged from 36.24 to 6339.54 snakes (Table 3; Fig. 4). Contrary to the SC estimator, abundance estimates from the REST estimator increased more with increasing lure attraction (increasing 43.1 times on average at the same camera density) than with increasing camera trap density (with no consistent pattern). Percent relative bias was lowest when there was no lure attraction, again with no consistent pattern by changing camera density (Table 3).

Similar to the SC estimator, CV also decreased with increasing lure attraction (an average of 84.8% from no to high lure attraction at the same camera density; Table 3). Increasing camera densities or rotating locations generally had lower CV. Results from the REST model had low coverage on average, varying between 0 to 43% coverage. Scenarios with no lure attraction were generally the only instances with coverage greater than 0. Convergence occurred in 100% of all simulations and scenarios. The camera trapping scenario using 8 rotating cameras at low levels of lure attraction had the closest estimate to truth (170.36 snakes with PRB = 41.97) with 6.24% CV, though HDPI contained truth in only 5% of the simulations.

Space to Event

Mean abundance estimates ranged from 142.83 to 5843.68 snakes (Table 3; Fig. 4). Similar to the REST estimator, abundance estimates from the STE estimator increased more with increasing lure attraction (increasing 23.4 times on average for a given camera density) as compared to increasing camera density (which showed a pattern of decreasing abundance within the same lure attraction level). Percent relative bias generally increased with increasing lure attraction and increasing camera densities or rotating locations.

Across all simulations, CV similarly decreased with increasing lure attraction (an average of 65.3% from no to high lure attraction at the same camera density; Table 3) and increasing or rotating camera density. Coverage was generally low, varying between 0 and 31% of simulations, but again only non-zero coverage was achieved in scenarios that had no lure attraction (Table 3). Model convergence was achieved for all simulations and scenarios. The camera trapping scenario using 8 static cameras with no lure attraction had the closest estimate to truth (142.83 snakes) with 16.34% CV, though HDPI contained truth only 25% of the simulations.

Instantaneous Sampling

Mean abundance estimates varied from 155.47 to 8809.61 snakes (Table 3; Fig. 4), which was the highest estimated abundance across all estimators. Again, abundance estimates increased more with increasing lure attraction (an average of 27.9 times within a camera trap density), and estimates showed no consistent pattern with increasing camera density. Percent relative bias was again higher with increasing lure attraction and at rotating or increasing camera densities (Table 3).

Similar to other estimators, CV decreased with increasing lure attraction (an average of 80.5% from no to high lure attraction at the same camera density, Table 3) and increasing or rotating camera density. Coverage was similarly low as well, varying between 0 and 27% of simulations within a scenario (Table 3). Only scenarios with no lure attraction had CIs that contained truth, and generally lower camera densities (8 static and rotating cameras) also had better coverage. The camera trapping scenario using 8 static cameras with no lure attraction had the closest estimate to truth (155.47 snakes) with 27% CV, though CI contained truth only 27% of the simulations.

Discussion

Wildlife managers require reliable (e.g., precise) information to inform their decisions. The value of such information is traded off against the cost of attaining it, and logistical challenges will increase costs. We sought reliable estimates of brown treesnake abundance while recognizing that the logistical challenges and resulting costs for hand- or trap-captures of snakes are substantial. Camera traps provide a lower-cost, broad-scale monitoring option but, in our system, require the use of lures in order to collect sufficient data and restrict analytical approaches to those based on non-uniquely identifiable individuals. We had the opportunity to assess the use of camera trapping and unmarked estimators to estimate abundance in a population of presumed size, an evaluation and comparison of these protocols and estimators that has rarely been done outside of computer simulations (Gilbert et al. 2020). The CP provided a study area specifically designed to contain a geographically closed population (here, 116 snakes of a size that would be sampled in mouse-lure snake traps), and previous studies within CP found similar abundances (e.g., 122 and 117 snakes; Tyrrell et al. 2009 and Christy et al. 2010 respectively). The brown treesnake density of 23 snakes/ha within CP is within the resonable range of snake densities found in Guam's forests (Rodda et al. 1999c) and is supported by a SCR analysis of marked individuals (Appendix S2).

We found that several of the approaches available for analyzing unmarked data from camera traps (SC, REST, STE, and IS estimators) did not return values that were accurate or precise. The average estimated abundance of snakes from the four estimators (from Table 2; N = 161.27) was about 1.4 times the presumed snake abundance within CP, and estimates ranged from 8.61 to 1061.52 snakes. All estimates were imprecise, with wide HDPIs (vague SC estimator) or those with narrower HDPI or CIs but that did not contain truth (informed SC, REST, STE, IS estimators). While model estimates always possess a degree of uncertainty, estimates with large levels of uncertainty, or estimates that consistently over- or underestimate truth, will not be useful when making management decisions, and even have the potential to be counter-productive (e.g., Moore and Kendall 2004). Our evaluation of different estimation approaches in a field setting is rare in wildlife studies and extremely important in invasive species management where abundance estimates can radically change the management actions selected (e.g., Januchowski-Hartley et al. 2011, Rout et al. 2017, Sofaer et al. 2018). Particularly for brown treesnakes, an abundance index may not be precise enough in order to make reliable management decisions due to the high level of predation risk a single individual presents

(Savidge 1987, Lardner et al. 2009, J.A. Savidge *pers. comm.*). Additionally, as the original founding population on Guam was only a few individuals (Richmond et al. 2015), precise abundance estimates will be needed to assess the success of suppression or eradication efforts.

Methods for estimating abundance in unmarked populations were developed to solve a challenging problem; in wildlife conservation and management, we want reliable abundance estimates for populations on which we frequently have very little information. Unmarked estimators are needed in many systems where animals cannot be identified or marked and recaptured in a reliable or cost-efficient manner (Pollock et al. 2002). Each available estimator relies on different data and assumptions (Table 1) and yet these estimators are similar in that they are based on either the rate of detections or the interval between detections (e.g., time or space between events) for abundance estimation. The relatedness of these metrics is important to understanding similarities in estimates often observed across estimators. For example, assuming a Poisson distribution with mean rate λ for the number of encounters at a trap implies the average duration between encounters is exponentially distributed with mean $1/\lambda$. Models with a Poisson-type distribution deal with the numbers of occurrences in a fixed unit of time or space (e.g., SC, counts in REST), and models with an exponential-type distribution deal with the time or space between occurrences of successive events (e.g., STE, staying time in REST model). Thus the estimators we used are somewhat interrelated, explaining why they frequently behaved similarly even though they can be quite dissimilar in the data collection protocols and species behavior required to meet assumptions (Chandler and Royle 2013, Moeller et al. 2018, Nakashima et al. 2018; Table 1).

One common assumption of several of these estimators that we violated is that animal movement is independent of camera traps (i.e., cameras do not change the behavior of individuals; Moeller et al. 2018, Nakashima et al. 2018). Specifically, the lures that cameras were pointed at (rather than the cameras themselves) clearly influenced snake behavior, as snakes would often spend substantial time trying to gain access to the mouse lure. Furthermore, we would argue that the use of lures could potentially lead to violation of the assumption that activity centers are the result of a homogenous spatial point process (Chandler and Royle 2013) as others have shown individual behavioral effects (e.g., trap-happiness or territoriality) can bias estimates from SCR estimators (note, Reich and Gardner 2014 found only a minimal bias).

Additional sources of bias can come from a high degree of home range overlap in the study species (e.g., brown treesnakes largely lack territoriality) and/or from animals clustering around lures, increasing the uncertainty in identifying unique individuals in photocapture events. Additionally, in situations where lure attraction or species movement ecology result in limited movement between cameras (i.e., at lower cameras densities in our simulation study), sufficient camera trap density on the landscape may be difficult to achieve in order for the SC estimator to perform well (i.e., to achieve a sufficient number of spatial recaptures; Chandler and Royle 2013). More investigation on these points are needed to pinpoint solutions for species that violate estimator assumptions or exhibit challenging life history and movement ecology. We contend that, if no lure or bait can be used in order to meet assumptions of these estimators, then detection events are likely to be exceedingly rare for many taxa (e.g., Karanth and Nichols 2011, du Preez et al. 2014, Peris et al. 2019). Particularly with herpetofauna, which do not use game trails and, in the case of arboreal species, which use the landscape as a three-dimensional space, obtaining sufficient captures can be challenging without the use of some means to direct and channel animal movement (e.g., Hobbs and Brehme 2017, Mills et al. 2019). However, lures paired with camera traps may better sample herpetofauna as compared to other traditional methods (e.g., Ariefiandy et al. 2013, Adams et al. 2017). For example, during this study, while brown treesnakes tended to probe the trap body for access to the mouse, they typically failed to find either of the trap entrances, and we caught only five brown treesnakes while obtaining 255 photo-captures. One challenge of applying the SC model (Chandler and Royle 2013) was that, as we used a live prey animal as a lure, snakes spent more time at traps and seemed to return to a trap to investigate (e.g., leaving the frame for one to a few 30-second time intervals before returning from the exact locations they appeared to exit). This made defining a photo-capture event particularly challenging, and sensitivity to the definition of an event in the SC framework should be further explored. In the case of herpetofauna “sit-and-wait” predators, the utility of obtaining abundance estimates using camera traps may improve if less-appealing scent lures are used as compared to live lures (so that sufficient photocaptures are still obtained but lure attraction is weaker).

As lure use is essentially unavoidable in our system, we used simulation to investigate how sensitive these estimators are to violations of the assumption that behaviors are not changed by traps. Again, no estimators produced abundance estimates that were reasonably accurate or precise. We found that all estimators were impacted by lure attraction, with estimates of abundance generally increasing with increasing lure attraction. Interestingly, the SC estimator was less sensitive to lure attraction (though estimates still increased on average), suggesting that this estimator may be less biased in this respect. Abundance estimates were inaccurate in nearly all simulations, with values ranging from 36.24 to 8809.61 individuals (or D = 8/ha to 1891/ha), an increase of nearly 24,209% as compared to the true abundance of 120 snakes. Yet lure attraction also increased photo-captures, highlighting the dilemma between obtaining sufficient camera trapping data and knowingly violating assumptions of estimators, which can drastically change abundance estimates.

Additionally, with only eight cameras, we were limited in how completely our study area could be sampled in a given survey. As other studies are also similarly limited in the number of cameras they can deploy, we wanted to assess if increased camera density could improve abundance estimates. From our simulations, we saw no clear benefit to increasing camera trap density based on results from these four estimators. There was no pattern of increasing accuracy or coverage from estimators using data collected from higher densities of cameras, and, more often, abundance estimates continued to increase with more camera traps used. Additionally, the presence of any lure attraction combined with increasing camera density led to increasingly inaccurate and imprecise estimates. The required use of lures to attract animals to camera traps could limit the usefulness of increasing camera trap density in populations of unmarked animals. Other limitations are also associated with increasing camera trap density. Beyond the cost of purchasing more camera traps, there are logistical limitations to processing the data generated by additional cameras. For many species, particularly ectothermic herpetofauna, motion-trigger camera traps do not reliably detect animals in the FOV, requiring the use of the time-lapse function or alternative triggering mechanisms (Hobbs and Brehme 2017, Siers et al. 2019). For our 45-day study, a single camera set to photograph every 30 seconds generated 64,800 photographs, resulting in 518,400 images across eight cameras. During a study of the same duration, 16, 24, and 48 cameras would generate 1,036,800, 1,555,200, and 3,110,400 images respectively. Camera trapping studies must rely on either extensive person-hours to manually process photographs or, increasingly, on partnerships with groups possessing machine-learning resources in order to automate processing and management of large photograph datasets (Norouzzadeh et al. 2018, Young et al. 2018).

There are several promising avenues for research and model development that could improve abundance estimation processes in our case study, and for herpetofauna with cryptic behavior more generally. Further work incorporating telemetry data can lead to a better understanding of how animal behavior (e.g., trap-specific responses such as trap avoidance, lure attraction; Zarnoch 1979, Meek et al. 2016) can impact abundance estimates based on camera trapping data, while also providing informed priors for certain model parameters. Particularly in the context of suppression and removal efforts that change brown treesnake densities, understanding the response of snakes to traps on the landscape will be important for abundance estimation. Development of alternate ways to obtain individual identity on cameras (e.g., reflective tags; Jordan et al. 2011) may also help improve the feasibility of obtaining reliable abundance estimates using camears. Integration of multiple monitoring methods may also improve estimation (Sollmann et al. 2013, Blanc et al. 2014, Popescu et al. 2014), allowing managers to make use of relatively inexpensive camera data by integrating it with smaller amounts of more expensive data sources to optimally balance reliability and cost.

We possessed information from an atypical situation where, with a presumed abundance, we could alter estimator priors and parameterizations to see if we could improve abundance estimates and better recover truth. However, for most studies, managers are dependent on abundance estimates from estimators with no ability to assess the accuracy or precision of values outside of simulations. We suggest that, similar to our approach, by comparing multiple abundance estimation approaches and looking for inconsistencies when changing parameters, more information can be obtained regarding the reliability of model estimates or at least the level of associated uncertainty that should be recognized while making management decisions. Our results also indicate that extreme caution should be used when interpreting estimates to make management decisions of great consequence on systems with little supplementary knowledge.

If extirpated species are to be reintroduced following efforts to reduce invasive predator abundance, decisions must be informed, intentional, and transparent as uncertainty is often high and the consequences of (in)action can be monumental (Converse et al. 2013, Fuller et al. 2020). Restoration efforts for degraded habitats impacted by invasive species must balance the reintroduction of native biodiversity with the eradication or suppression of invasive species. Decisions about the deployment of resources and budgeting of time and money often rely on changes in demographic rates or abundance of both native and introduced species that trigger management responses (Armstrong et al. 2006, Garrett et al. 2007). On Guam, abundance estimates of brown treesnakes in areas targeted for suppression directly contribute to evaluating suppression success, budgeting money for continued suppression efforts, and assessing feasibility of vertebrate reintroductions. We found that, given the management decisions contingent on abundance estimates of brown treesnakes, camera traps and unmarked estimators alone are likely insufficient to provide the information necessary for management decisions.

Acknowledgments

We thank the Office of Insular Affairs and Joint Region Marianas for providing support for this project, and M. Hall (Brown Treesnake Program Manager, Naval Facilities Engineering Command Marianas) for providing logistical support. We thank Andersen Air Force Base for granting field access to the study site. We would like to profoundly thank all of the field biologists who helped collect these data with a special acknowledgement to the very patient photograph processors for this project, particularly P. Barnhart, T. Hinkle, M. Hogan, E. Holldorf, J. Kaseman, C. Robinson, and M. Viernes. We additionally thank R. Chandler and B. Gerber for modeling insights. Snake and mouse handling was conducted as per protocols of the U.S. Geological Survey (FORT IACUC 2013-13) and Colorado State University (IACUC-15-5892A) Institutional Animal Care and Use Committees. The scientific results and conclusions, as well as any views or opinions expressed herein, are those of the author(s) and do not necessarily reflect those of NOAA or the Department of Commerce. Any use of trade, firm, or product names is for descriptive purposes only and does not imply endorsement by the U.S. Government. Data analyzed in this study are available as a USGS data release (Amburgey et al. 2021).

Supporting Information

Additional supporting information may be found online at: [link to be added in production]

Open Research

Data analyzed in this study are available as a USGS data release (Amburgey et al. 2021) on ScienceBase: https://doi.org/10.5066/P9JV1QU5

Literature Cited

Adams, C. S., W. A. Ryberg, T. J. Hibbits, V. L. Pierce, J. B. Pierce, and D. C. Rudolph. 2017. Evaluating effectiveness and cost of time-lapse triggered camera trapping techniques to detect terrestrial squamate diversity. Herpetological Review 48:44–48.

Amburgey, S.M., A.A. Yackel Adams, and S.J. Converse. 2021. Camera trap data of Brown Treesnakes at mouse-lure traps on Guam, 2015: U.S. Geological Survey data release, https://doi.org/10.5066/P9JV1QU5.

Ariefiandy, A., D. Purwandana, A. Seno, C. Ciofi, and T. S. Jessop. 2013. Can camera traps monitor Komodo dragons a large ectothermic predaotr? PLoS ONE 8:e58800.

Armstrong, D. P., E. H. Raeburn, R. M. Lewis, and D. Ravine. 2006. Modeling Vital Rates of a Reintroduced New Zealand Robin Population as a Function of Predator Control. Journal of Wildlife Management 70:1028–1036.

Armstrong, D. P., and P. J. Seddon. 2008. Directions in reintroduction biology. Trends in Ecology and Evolution 23:20–25.

Blanc, L., E. Marboutin, S. Gatti, F. Zimmermann, and O. Gimenez. 2014. Improving abundance estimation by combining capture re-capture and occupancy data: example with a large carnivore. Journal of Applied Ecology 51:1733–1739.

Bohmann, K., A. Evans, M. T. P. Gilbert, G. R. Carvalho, S. Creer, M. Knapp, D. W. Yu, and M. de Bruyn. 2014. Environmental DNA for wildlife biology and biodiversity monitoring. Trends in Ecology and Evolution 29:358–367.

Brillinger, D. R., H. K. Preisler, A. A. Ager, and J. Kie. 2012. The use of potential functions in modelling animal movement. Selected Works of David Brillinger, pp. 385–409. Springer, Berkley, CA, USA.

Brodie, J. F. 2006. An Experimentally Determined Persistence-Rate Correction Factor for Scat-Based Abundance Indices. Wildlife Society Bulletin 34:1216–1219.

Chandler, R. B., and J. A. Royle. 2013. Spatially explicit models for inference about density in unmarked or partially marked populations. Annals of Applied Statistics 7:936–954.

Christy, M. T., A. A. Yackel Adams, G. H. Rodda, J. A. Savidge, and C. L. Tyrrell. 2010. Modelling detection probabilities to evaluate management and control tools for an invasive species. Journal of Applied Ecology 47:106–113.

Converse, S. J., C. T. Moore, and D. P. Armstrong. 2013. Demographics of reintroduced populations: Estimation, modeling, and decision analysis. Journal of Wildlife Management 77:1081–1093.

Cusack, J. J., A. J. Dickman, J. M. Rowcliffe, C. Carbone, D. W. Macdonald, and T. Coulson. 2015. Random versus game trail-based camera trap placement strategy for monitoring terrestrial mammal communities. PLoS One 10:e0126373.

Dénes, F. V., L. F. Silveira, and S. R. Beissinger. 2015. Estimating abundance of unmarked animal populations: Accounting for imperfect detection and other sources of zero inflation. Methods in Ecology and Evolution 6:543–556.

du Preez, B. D., A. J. Loveridge, and D. W. Macdonald. 2014. To bait or not to bait: A comparison of camera-trapping methods for estimating leopard *Panthera pardus* density. Biological Conservation 176:153–161.

Fritts, T. H. 1988. The brown tree snake, *Boiga irregularis*, a threat to Pacific Islands. Fish and Wildlife Service Biological Report 88:1–37.

Fuller, A. K., D. J. Decker, M. V. Schiavone, and A. B. Forstchen. 2020. Ratcheting up rigor in wildlife management decision making. Wildlife Society Bulletin 44:29–41.

Garrett, L. J. H., C. G. Jones, A. Cristinacce, and D. J. Bell. 2007. Competition or co-existence of reintroduced, critically endangered Mauritius fodies and invasive Madagascar fodies in lowland Mauritius? Biological Conservation 140:19–28.

Gelman, A., J. B. Carlin, H. S. Stern, D. B. Dunson, A. Vehtari, and D. B. Rubin. 2013. Bayesian data analysis. 3rd Edition. pp. 287. Chapman & Hall, Boca Raton, FL, USA.

Gerber, B. D., and R. R. Parmenter. 2015. Spatial capture-recapture model performance with well-estimated small-mammal densities. Ecological Applications 25:695–705.

Gilbert, N. A., J. D. Clare, J. L. Stenglein, and B. Zuckerberg. 2020. Abundance estimation methods for unmarked animals with camera traps. Conservation Biology. Early View.

Guam Coastal Management Program. 2013. Contour lines (50-meter interval). Bureau of Statistics and Plans. Available at http://north.hydroguam.net/gis_download.php.

Hobbs, M. T., and C. S. Brehme. 2017. An improved camera trap for amphibians, reptiles, small mammals, and large invertebrates. PLoS ONE 12:1–15.

IUCN. 2001. IUCN Red List categories and criteria (IUCN Species Survival Commission, Ed.; Version 3.). IUCN.

Jachowski, D., J. Millspaugh, P. Angermeier, and R. Slotow. (Eds.). 2016. Reintroduction of fish and wildlife populations (1st ed.). University of California Press, Berkley, CA, USA.

Januchowski-Hartley, S. R., P. Visconti, and R. L. Pressey. 2011. A systematic approach for prioritizing multiple management actions for invasive species. Biological Invasions 13:1241–1253.

Jordan, M. J., R. H. Barrett, and K. L. Purcell. 2011. Camera trapping estimates of density and survival of fishers *Martes pennant*. Wildlife Biology 17:266–276.

Karanth, K. U., and J. D. Nichols. 1998. Estimation of tiger densities in India using photographic captures and recaptures. Ecology 79:2852–2862.

Karanth, K. U., and J. D. Nichols. 2011. Estimating tiger abundance from camera trap data: Field surveys and analytical issues. In: A.F. O'Connell, J.D. Nichols, K. U. Karanth (Eds). Camera Traps in Animal Ecology. Springer, Tokyo, Japan.

Kellner, K. 2018. jagsUI: A Wrapper Around "rjags" to Streamline "JAGS" Analyses. (R package version 1.5.0). https://cran.r-project.org/package=jagsUI

Kraus, F. 2009. Alien Reptiles and Amphibians: A Scientific Compendium and Analysis. Springer Netherlands.

Kraus, F. 2015. Impacts from Invasive Reptiles and Amphibians. Annual Review of Ecology, Evolution, and Systematics 46:75–97.

Lardner, B., J. A. Savidge, G. H. Rodda, and R. N. Reed. 2009. Prey Preferences and Prey Acceptance in Juvenile Brown Treesnakes (*Boiga irregularis*). Herpetological Conservation and Biology 4:313–323.

Lardner, B., A. A. Yackel Adams, G. H. Rodda, R. N. Reed, and C. S. Clark. 2013. Effectiveness of bait tubes for brown treesnake control on Guam. Wildlife Society Bulletin 37:664–673.

Larson, D. L., L. Phillips-Mao, G. Quiram, L. Sharpe, R. Stark, S. Sugita, and A. Weiler. 2011. A framework for sustainable invasive species management: Environmental, social, and economic objectives. Journal of Environmental Management 92:14–22.

Link, W. A. 2013. A cautionary note on the discrete uniform prior for the binomial N: Reply. Ecology 95:2677–2679.

Link, W. A., S. J. Converse, A. A. Yackel Adams, and N. J. Hostetter. 2018. Analysis of Population Change and Movement Using Robust Design Removal Data. Journal of Agricultural, Biological, and Environmental Statistics 23:463–477.

Maguire, L. A. 2004. What Can Decision Analysis Do for Invasive Species Management ? Risk Analysis 24:859–868.

McClintock, B. T., and Michelot, T. 2018. momentuHMM: R package for analysis of telemetry data using generalized multivariate hidden Markov models of animal movement. Methods in Ecology and Evolution 9:1518–1530.

Meek, P., G. Ballard, P. Fleming, and G. Falzon. 2016. Are we getting the full picture? Animal responses to camera traps and implications for predator studies. Ecology and Evolution 6:3216–3225.

Mills, D., J. Fattebert, L. Hunter, and R. Slotow. 2019. Maximising camera trap data: Using attractants to improve detection of elusive species in multi-species surveys. PLoS One 14:e0216447.

Mitchell, M. S., H. Cooley, J. A. Gude, J. Kolbe, J. J. Nowak, K. M. Proffitt, S. N. Sells, and M. Thompson. 2018. Distinguishing values from science in decision making: Setting harvest quotas for mountain lions in Montana. Wildlife Society Bulletin 42:13–21.

Moeller, A. K., P. M. Lukacs, and J. S. Horne. 2018. Three novel methods to estimate abundance of unmarked animals using remote cameras. Ecosphere 9:e02331.

Mooney, H. A., and R. J. Hobbs (Eds.). 2000. Invasive Species in a Changing World. Island Press. Washington D.C., USA.

Moore, C. T., and W. L. Kendall. 2004. Costs of detection bias in index-based population monitoring. Animal Biodiversity and Conservation 27:287–296.

Nafus, M G., A. A. Yackel Adams, P. E. Klug, G. H. Rodda. 2018. Habitat type and structure affect trap capture success of an invasive snake across variable densities. Ecosphere 9:e02339.

Nakashima, Y., K. Fukasawa, and H. Samejima. 2018. Estimating animal density without individual recognition using information derivable exclusively from camera traps. Journal of Applied Ecology 55:735–744.

Nichols, J. D., M. C. Runge, F. A. Johnson, and B. K. Williams. 2007. Adaptive harvest management of North American waterfowl populations: A brief history and future prospects. Journal of Ornithology 148:343–349.

Norouzzadeh, M. S., A. Nguyen, M. Kosmala, A. Swanson, M. S. Palmer, C. Packer, and J. Clune. 2018. Automatically identifying, counting, and describing wild animals in camera-trap images with deep learning. Proceedings of the National Academy of Sciences of the United States of America 115:E5716–E5725.

O'Connell, A. F., J. D. Nichols, K. U. Karanth (Eds). 2011. Camera Traps in Animal Ecology. Springer, Tokyo, Japan.

Pejchar, L., and H. A. Mooney. 2010. The Impact of Invasive Alien Species on Ecosystem Services and Human Well-being. Trends in Ecology and Evolution 24:497–504.

Peris, A., F. Closa-Sebastiá, I. Marco, E. Serrano, and E. Casas-Díaz. 2019. Baiting improves wild boar population size estimates by camera trapping. Mammalian Biology 98:28–35.

Perry, G., E. W. Campbell, G. H. Rodda, and T. H. Fritts. 1998. Managing island biotas: brown tree snake control using barrier technology. In: R. O. Baker and A. C. Crabb (Eds).

Proceedings of the 18th Vertebrate Pest Conference. University of California Press, Davis, CA, USA.

Pimentel, D., R. Zuniga, and D. Morrison. 2005. Update on the environmental and economic costs associated with alien-invasive species in the United States. Ecological Economics 52:273–288.

Plummer, M. 2003. JAGS: A program for analysis of Bayesian graphical models using Gibbs sampling. Proceedings of the 3rd International Workshop on Distributed Statistical Computing:1–8.

Pollock, K. H., J. D. Nichols, T. R. Simons, G. L. Farnsworth, L. L. Bailey, and J. R. Sauer. 2002. Large scale wildlife monitoring studies: Statistical methods for design and analysis. Environmetrics 13:105–119.

Popescu, V. D., P. de Valpine, and R. A. Sweitzer. 2014. Testing the consistency of wildlife data types before combining them: a case of camera traps and telemetry. Ecology and Evolution 4:933–943.

Ramsey, D. S. L., J. Parkes, and S. A. Morrison. 2009. Quantifying Eradication Success: the Removal of Feral Pigs from Santa Cruz Island, California. Conservation Biology 23:449–459.

R Core Team. 2019. R: A language and environment for statistical computing. R Foundation for Statistical Computing. http://www.R-project.org/

Reconyx Inc. 2013. Reconyx Hyperfire Instruction Manual:1–183.

Reich, B. J., and B. Gardner. 2014. A spatial capture-recapture model for territorial species. Environmetrics 25: 630-637.

Reynolds, J. H., W. L. Thompson, and B. Russell. 2011. Planning for success: Identifying effective and efficient survey designs for monitoring. Biological Conservation 144:1278–1284.

Richmond, J. Q., D. A. Woods, J. W. Stanford, and R. N. Fisher. 2015. Testing for multiple invasion routes and source populations for the invasive brown treesnake (Boiga irregularis) on Guam: implications for pest management. Biological Invasions 17: 337-349.

Rodda, G. H., T. H. Fritts, and P. J. Conry. 1992. Origin and population growth of the brown tree snake, *Boiga irregularis*, on Guam. Pacific Science 46:46–57.

Rodda, G. H., T. H. Fritts, C. S. Clark, S. W. Gotte, and D. Chiszar. 1999a. A state-of-the-art trap for the brown treesnake. In: G. H. Rodda, Y. Sawai, D. Chiszar, and H. Tanaka (Eds). Problem snake management: the habu and the brown treesnake. Cornell University Press, Ithaca, New York, USA.

Rodda, G. H., T. H. Fritts, M. J. McCoid, and E. W. Campbell III. 1999b. An overview of the biology of the brown treesnake (*Boiga irregularis*), a costly introduced pest on Pacific islands. In: G. H. Rodda, Y. Sawai, D. Chiszar, and H. Tanaka (Eds). Problem snake management: the habu and the brown treesnake. Cornell University Press, Ithaca, New York, USA.

Rodda, G. H., M. J. McCoid, T. H. Fritts, and E. W. Campbell III. 1999c. Population Trends and Limiting Factors in *Boiga irregularis*. In: G. H. Rodda, Y. Sawai, D. Chiszar, H. Tanaka. (Eds). Problem Snake Management: The Habu and the Brown Treesnake. Cornell University Press, Ithaca, NY.

Rodda, G. H., and J. A. Savidge. 2007. Biology and Impacts of Pacific Island Invasive Species. 2. *Boiga irregularis*, the Brown Tree Snake (Reptilia: Colubridae). Pacific Science 61:307–324.

Rodda, G. H., J. A. Savidge, C. L. Tyrrell, M. T. Christy, and A. R. Ellingson. 2007. Size Bias in Visual Searches and Trapping of Brown Treesnakes on Guam. Journal of Wildlife Management 71:656–661.

Rout, T. M., C. E. Hauser, M. A. McCarthy, and J. L. Moore. 2017. Adaptive management improves decisions about where to search for invasive species. Biological Conservation 212:249–255.

Rovero, F., F. Zimmermann, D. Berzi, and P. Meek. 2013. "Which camera trap type and how many do I need?" A review of camera features and study designs for a range of wildlife research applications. Hystrix, the Italian Journal of Mammalogy 24:148–156.

Rovero, F., and F. Zimmermann. 2016. Camera trapping for wildlife research. Pelagic Publishing Ltd, Exeter, UK.

Rowcliffe, J. M., J. Field, S. T. Turvey, and C. Carbone. 2008. Estimating animal density using camera traps without the need for individual recognition. Journal of Applied Ecology 45:1228–1236.

Royle, J. A., and B. Gardner. 2011. Hierarchical Spatial Capture-Recapture Models for Estimating Density from Trapping Arrays. In: A. F. O'Connell, J. D. Nichols, and K. U. Karanth (Eds). Camera Traps in Animal Ecology: Methods and Analyses. pp. 163–190. Springer, Berkley, CA, USA.

Royle, J. A., R. B. Chandler, R. Sollmann, and B. Gardner. 2014. Spatial Capture-Recapture. Academic Press.

Savidge, J. A. 1987. Extinction of an island forest avifauna by an introduced snake. Ecology 68:660–668.

Savidge, J. A. 1988. Food Habits of *Boiga irregularis*, an Introduced Predator on Guam. Journal of Herpetology 22:275–282.

Siers, S. R., J. A. Savidge, and R. N. Reed. 2014. Invasive Brown Treesnake Movements at Road Edges Indicate Road-Crossing Avoidance. Journal of Herpetology 48:500–505.

Siers, S. R., A. A. Yackel Adams, and R. N. Reed. 2018. Behavioral differences following ingestion of large meals and consequences for management of a harmful invasive snake: A field experiment. Ecology and Evolution 8:10075–10093.

Siers, S. S., A. B. Shiels, C. G. Payne, F. M. Chlarson, C. S. Clark, and S. M. Mosher. 2019. Photographic validation of target versus nontarget take of brown treesnake baits. Wildlife Society Bulletin 43:752–759.

Siers, S. R., A. B. Shiels, and P. D. Barnhart. 2020. Invasive snake activity before and after automated aerial baiting. Journal of Wildlife Management 84:256–267.

Sofaer, H. R., C. S. Jarnevich, and I.S. Pearse. 2018. The relationship between invader abundance and impact. Ecosphere 9:e02415.

Tracey, J. P., P. J. S. Fleming, and G. J. Melville. 2005. Does variable probability of detection compromise the use of indices in aerial surveys of medium-sized mammals? Wildlife Research 32:245–252.

Tyrrell, C. L., M. T. Christy, G. H. Rodda, A. A. Yackel Adams, A. R. Ellingson, J. A. Savidge, K. Dean-Bradley, and R. Bischof. 2009. Evaluation of trap capture in a geographically closed population of brown treesnakes on Guam. Journal of Applied Ecology 46:128–135.

Waits, L. P., and D. Paetkau. 2005. Noninvasive Genetic Sampling Tools for Wildlife Biologists: a Review of Applications and Recommendations for Accurate Data Collection. Journal of Wildlife Management 69:1419–1433.

Williams, R., and L. Thomas. 2009. Cost-effective abundance estimation of rare animals: Testing performance of small-boat surveys for killer whales in British Columbia. Biological Conservation 142:1542–1547.

Yackel Adams, A. A., M. G. Nafus, P. E. Klug, B. Lardner, M. J. Mazurek, J. A. Savidge, and R. N. Reed. 2019. Contact rates with nesting birds before and after invasive snake removal: Estimating the effects of trap-based control. NeoBiota 49:1–17.

Young, S., J. Rode-Margono, and R. Amin. 2018. Software to facilitate and streamline camera trap data management: A review. Ecology and Evolution 8:9947–9957.

Zarnoch, S. J. 1979. Simulation of effects of learned trap response on three estimators of population size. The Journal of Wildlife Management 43:474–483.

Zimmermann, F., C. Breitenmoser-Würsten, A. Molinari-Jobin, U. Breitenmoser. 2013. Optimizing the size of the area surveyed for monitoring a Eurasian lynx (*Lynx lynx* Linnaeus, 1758) population in the Swiss Alps by means of photographic capture-recapture. Integrative Zoology 8:232–243.

Table 1. Summary of the information required, assumptions, and original citation of the estimators for abundance estimation in unmarked populations that we used for a population of brown treesnakes. Field of view (FOV) indicates the area in front of a camera trap. We discuss these estimators in the context of closed population abundance estimation, which assumes demographic closure.

Model	Data Requirements	Assumptions	Summary
Spatial Count (SC; Chandler and Royle, 2013)	Count data; Spatially referenced traps; Traps in close spatial proximity	Stationary activity centers; No territoriality (i.e., activity centers do not alter animal movement); No temporal correlations in observations	Estimates abundance using the spatial pattern of animal encounters across the state space.
Random Encounter and Staying Time (REST; Nakashima et al., 2018)	Count data; Area of FOV; Motion-triggered video or short-interval time-lapse photographs in order to calculate staying time in the FOV	Perfect detection within FOV; Random camera placement; No temporal or spatial correlations in observations; Animal movement is random and independent of cameras; Staying time follows parametric distribution (i.e., no long periods of inactivity)	Estimates abundance as a function of the time animals stay in front of cameras, thus inferring how they move around the landscape.
Space to Event (STE; Moeller et al., 2018)	Count data; Area of FOV; Depth of FOV standardized to landmark; Time-lapse photographs to allow instantaneous sample of all cameras at defined time	Geographic (at sampling frame level) closure; Perfect detection within FOV (extension for imperfect detection exists); Random camera placement; No spatial or temporal correlation in observations; Animal movement is random and	Estimates abundance as a function of the total area searched until an animal is encountered within a FOV.

		independent of cameras	
Instantaneous Sampling (IS; Moeller et al., 2018)	Count data; Area of FOV; Depth of FOV standardized to landmark; Time-lapse photographs to allow instantaneous sample of all cameras at defined time	Geographic (at sampling frame level) closure; Perfect detection within FOV (extension for imperfect detection exists); Random camera placement; No spatial or temporal correlation in observations; Animal movement is random and independent of cameras; Accurate counts of animals	Estimates abundance as the total number of animal encounters at each camera at each instantaneous sample as fixed-area repeat counts.

Table 2. Estimated density (D; per ha), median and mean snake abundance (N_{mode} and N_{mean}), and model specifications fit for all estimators (SC = Spatial Count, REST = Random Encounter and Staying Time, STE = Space to Event, and IS = Instantaneous Sampling). Q2.5 and Q97.5 represent 2.5% and 97.5% highest density posterior intervals (HDPI) for all abundance values except the IS estimator where values represent confidence intervals obtained by bootstrapping. The parameters from the SC model using vague priors for σ and ψ were only identifiable at M = 1000. The presumed abundance within the Closed Population (CP) is 116 snakes (D = 23/ha), which is supported by results from a traditional spatial capture-recapture (SCR) estimator (124.35 snakes, HDPI = 110, 140). The STE and IS approaches were unchanged from their original formulations (i.e., the default).

Estimator	D	N_{mode}	N_{mean}	Q2.5	Q97.5
SC					
M = 1000					
σ ~ *Uniform* (0, 50), ψ ~ *Uniform* (0, 1)	34	80	167.83	9	546
M = 500					
σ ~ *Gamma* (274.69, 7.27), ψ ~ *Uniform* (0, 1)	2	7.97	10.11	4	18
σ ~ *Gamma* (274.69, 7.27), ψ ~ *Beta* (1e-6, 1)	2	5.96	8.61	4	15
σ ~ *Uniform* (0, 50), ψ ~ *Beta* (1e-6, 1)	15	57.65	74.23	7	174
REST					
Activity proportion = 0.2	212	1060.19	1061.52	863	1275
Activity proportion = 0.4	110	513.97	529.90	424	637
Activity proportion = 0.6	71	348.06	352.80	287	425
Activity proportion = 0.8	53	259.66	265.35	217	320
Activity proportion = 1	43	200.36	212.64	172	256
STE					
Default	38	183.55	191.65	152	238
IS					
Default	43	212.67	212.11	168	272

Table 3. Simulation results for each estimator at each camera density and setup (Scenario) and lure attraction level. We report the mode and mean of the number of snakes ($N_{mode,}$ N_{mean}), the percent relative bias in abundance (PRB), and the percent coefficient of variation (CV). We also report the percentage of simulations whose 95% HDPI or confidence intervals contained the true abundance of snakes (Coverage) and whose Gelman-Rubin statistic indicated adequate mixing ($\hat{R} < 1.1$; not applicable to the IS estimator). For most estimators, the number of converged simulations was 100; however, for the SC estimator, N_{mode}, $N_{mean,}$ PRB, CV, and Coverage were calculated using only those simulations with parameter estimates that converged. True N was 120 simulated snakes (D = 26/ha).

Scenario	Attraction	D	N_{mode}	N_{mean}	PRB	CV	Coverage	$\hat{R} < 1.1$
SC								
8 cameras, rotating placement	No	42	101.05	195.68	63.07	58.75	86	100
8 cameras, rotating placement	Low	52	175.96	241.17	100.98	49.06	78	93
8 cameras, rotating placement	High	44	172.75	204.41	70.34	46.88	82	93
8 cameras, static placement	No	13	18.72	60.10	-49.92	78.05	52	98
8 cameras, static placement	Low	15	26.97	69.15	-42.38	58.91	31	98
8 cameras, static placement	High	9	34.56	43.67	-63.61	45.69	12	99
16 cameras, static placement	No	27	45.48	127.99	6.65	76.50	85	99
16 cameras, static placement	Low	27	62.68	126.20	5.16	61.78	73	86
16 cameras, static placement	High	31	100.06	145.92	21.60	50.12	82	85
24 cameras, static placement	No	33	66.08	153.40	27.84	71.70	86	88
24 cameras, static placement	Low	35	108.35	161.44	34.53	57.03	80	82
24 cameras, static placement	High	58	256.31	271.01	125.84	36.78	51	87
48 cameras, static placement	No	58	229.47	270.51	125.43	46.37	60	93
48 cameras, static placement	Low	45	148.28	209.64	74.70	48.98	53	63

48 cameras, static placement	High	57	226.37	266.97	122.48	32.84	38	77
REST								
8 cameras, rotating placement	No	8	34.84	36.24	-69.80	16.63	0	100
8 cameras, rotating placement	Low	37	169.33	170.36	41.97	6.24	5	100
8 cameras, rotating placement	High	391	1821.74	1822.81	1419.01	1.95	0	100
8 cameras, static placement	No	38	171.75	179.12	49.27	22.27	43	100
8 cameras, static placement	Low	183	849.99	852.10	610.08	7.21	0	100
8 cameras, static placement	High	1140	5313.11	5313.16	4327.63	2.83	0	100
16 cameras, static placement	No	15	66.94	68.39	-43.01	12.73	17	100
16 cameras, static placement	Low	66	306.887	307.20	156.00	4.74	0	100
16 cameras, static placement	High	1361	6339.82	6339.54	5182.95	1.83	0	100
24 cameras, static placement	No	47	217.08	220.08	83.40	9.70	18	100
24 cameras, static placement	Low	205	953.68	953.29	694.41	3.78	0	100
24 cameras, static placement	High	1185	554.26	5522.70	4502.25	1.60	0	100
48 cameras, static placement	No	44	201.91	202.69	68.91	6.80	5	100
48 cameras, static placement	Low	166	771.34	772.14	543.45	2.93	0	100
48 cameras, static placement	High	770	3588.51	3589.88	2891.57	1.42	0	100
STE								
8 cameras, rotating placement	No	38	173.37	175.18	45.98	12.64	31	100
8 cameras, rotating placement	Low	158	738.69	738.35	515.29	6.25	0	100
8 cameras, rotating placement	High	1254	5846.51	5843.68	4769.73	3.20	0	100
8 cameras, static placement	No	31	140.62	142.83	19.02	16.34	25	100

8 cameras, static placement	Low	134	624.04	624.42	420.35	7.03	0	100
8 cameras, static placement	High	776	3619.16	3616.04	2913.36	3.54	0	100
16 cameras, static placement	No	38	174.25	175.29	46.072	9.80	18	100
16 cameras, static placement	Low	151	705.30	703.83	486.52	4.98	0	100
16 cameras, static placement	High	917	4268.83	4273.93	3461.61	3.13	0	100
24 cameras, static placement	No	41	188.58	189.71	58.09	7.66	17	100
24 cameras, static placement	Low	155	721.79	722.27	501.89	4.25	0	100
24 cameras, static placement	High	811	3779.89	3778.32	3048.60	3.08	0	100
48 cameras, static placement	No	38	178.72	179.30	49.42	5.62	10	100
48 cameras, static placement	Low	126	586.05	586.77	388.97	3.69	0	100
48 cameras, static placement	High	541	2518.89	2520.85	2000.71	3.06	0	100
IS								
8 cameras, rotating placement	No	42	192.54	193.66	61.38	12.71	27	NA
8 cameras, rotating placement	Low	180	834.87	837.83	598.19	5.89	0	NA
8 cameras, rotating placement	High	1891	8819.27	8809.61	7241.34	2.27	0	NA
8 cameras, static placement	No	33	152.84	155.47	29.56	16.46	27	NA
8 cameras, static placement	Low	149	695.56	696.15	480.12	6.72	0	NA
8 cameras, static placement	High	918	4277.94	4276.36	3463.64	2.65	0	NA
16 cameras, static placement	No	39	182.94	182.49	52.07	9.53	15	NA
16 cameras, static placement	Low	162	751.93	753.75	528.13	4.40	0	NA
16 cameras, static placement	High	1091	5079.84	5081.44	4134.54	1.69	0	NA
24 cameras, static placement	No	42	193.60	194.50	62.09	7.26	18	NA

24 cameras, static placement	Low	167	777.04	776.39	546.99	3.56	0	NA
24 cameras, static placement	High	950	4427.78	4427.50	3589.59	1.49	0	NA
48 cameras, static placement	No	39	181.15	181.07	50.96	5.16	8	NA
48 cameras, static placement	Low	135	631.27	630.65	426.06	2.74	0	NA
48 cameras, static placement	High	617	2874.45	2872.84	2295.37	1.30	0	NA

Figure 1. The study area located on the island of Guam, (A) located in the Pacific Ocean north of Papua New Guinea. (B) Guam is the southernmost island of the Marianas, with the closed population (CP) study area located on the northern tip of the island (C; orange diamond, not to scale).

Figure 2. The study area (the closed population, CP) and trapping design for the camera study. (A) Thirteen trapping transects, each with thirteen coordinate points, formed a grid throughout CP. Traps with cameras are highlighted, with color coordinating to the session at which traps were deployed (eight cameras at a time). To eliminate a pathway for snake movement, a buffer of removed vegetation exists around the outer and inner edge of the fence-line, which is visible on a 50-m digital elevation map (Guam Coastal Management Program, 2013). (B) The fence possessed a bulge on either side to prevent snakes from climbing into or out of CP. (C) A cropped photograph from a camera trap shows a brown treesnake inspecting the trap containing the caged mouse lure.

Figure 3. Comparison of abundance and density estimates from the four models evaluated (IS = Instantaneous Sampling, REST = Random Encounter and Staying Time, SC = Spatial Count, STE = Space to Event). The presumed abundance and density is represented by the dashed line. Error bars represent 2.5% and 97.5% highest density posterior intervals for all abundance values except the IS estimator where values represent confidence intervals obtained by bootstrapping. We included two estimates from the REST model, one from the model using the *a prior* assumption of an activity proportion (activ) of 0.6 and one that achieved the closest estimate to the well-estimated number of snakes where activ = 1. We included three estimates from the SC model (where $M = 500$), showing the three main parameterizations of the model priors used (1^{st} = vague σ and informed ψ, 2^{nd} = informed σ and vague ψ, and 3^{rd} = vague σ and ψ; Table 2). Additionally, we included a fourth SC estimate (where $M = 1000$) for the parameterization of vague σ and ψ.

Figure 4. Comparison of abundance estimates across simulations of each camera trapping scenario for the four estimators (IS = Instantaneous Sampling, REST = Random Encounter and Staying Time, SC = Spatial Count, STE = Space to Event). Values were calculated from 100 simulations except for the SC estimator where we used only those simulations with abundance estimates that converged. Camera densities increased from 8 static or rotating cameras to 48 static cameras (top to bottom panels) while lure attraction was absent (No lure) to high (left to right panels). Boxplots include median (darker line) abundance within the interquartile range (IQR; box), the largest and smallest values within 1.5*IQR (whiskers), and outliers (points). True simulated abundance (120 snakes) is indicated as a dashed line.

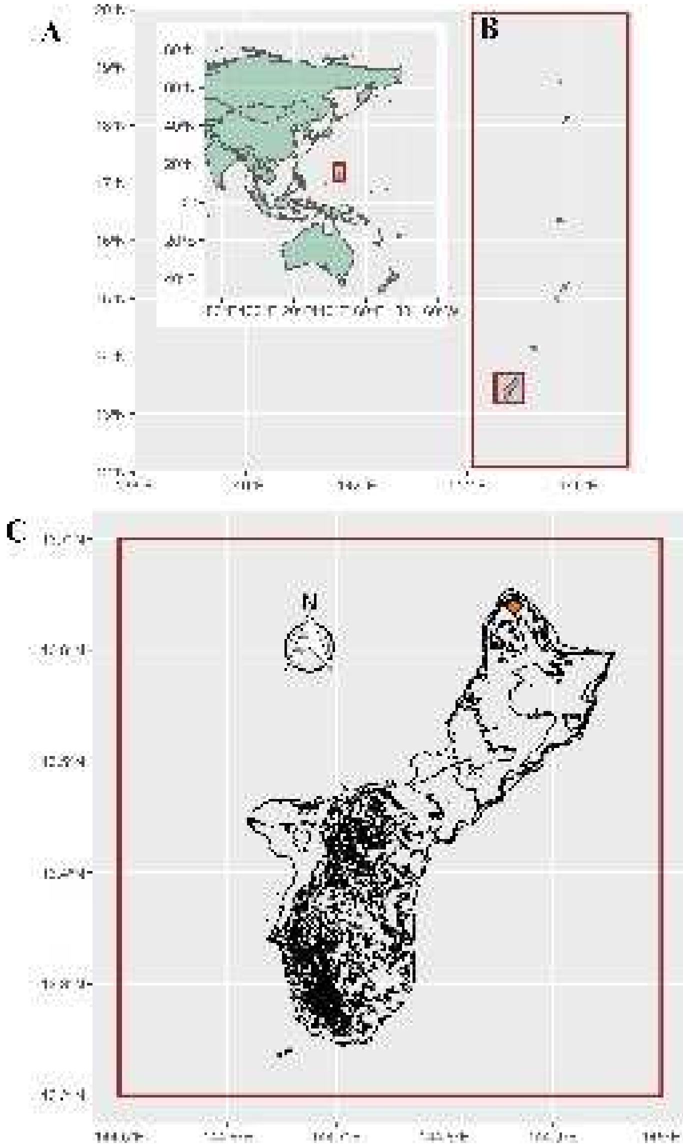

eap_2410_f1.png

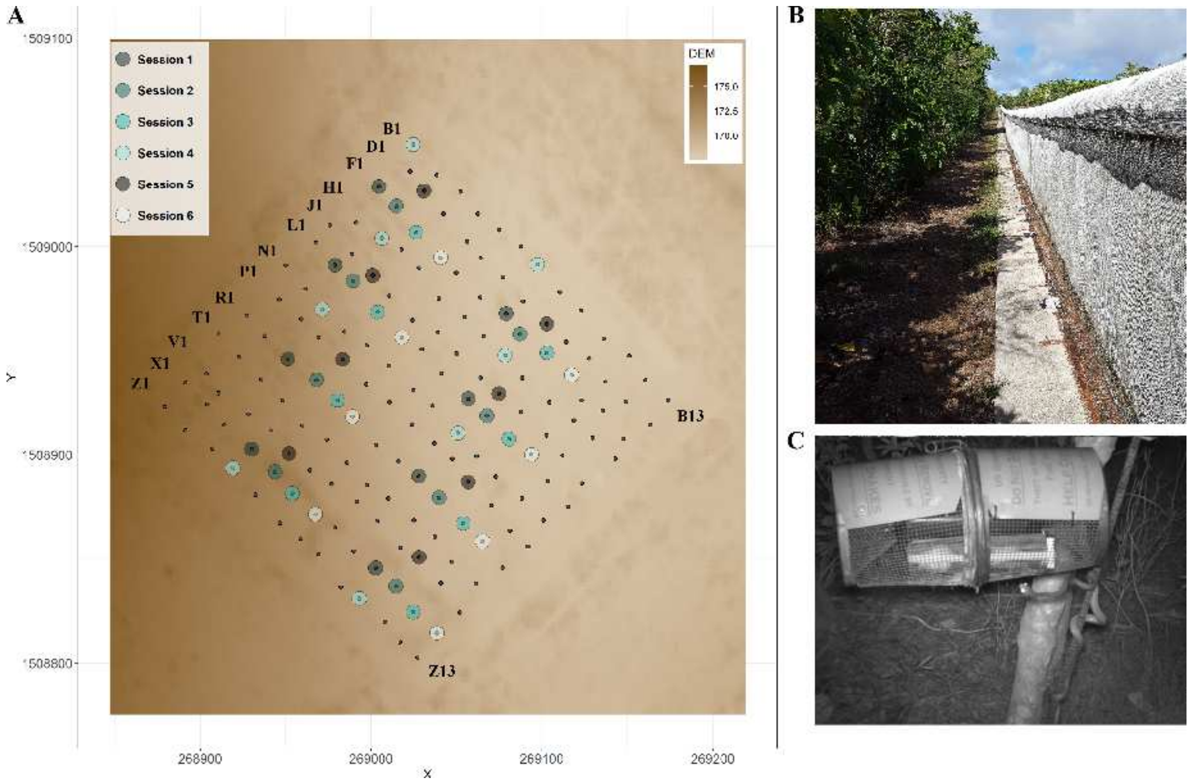

eap_2410_f2.png

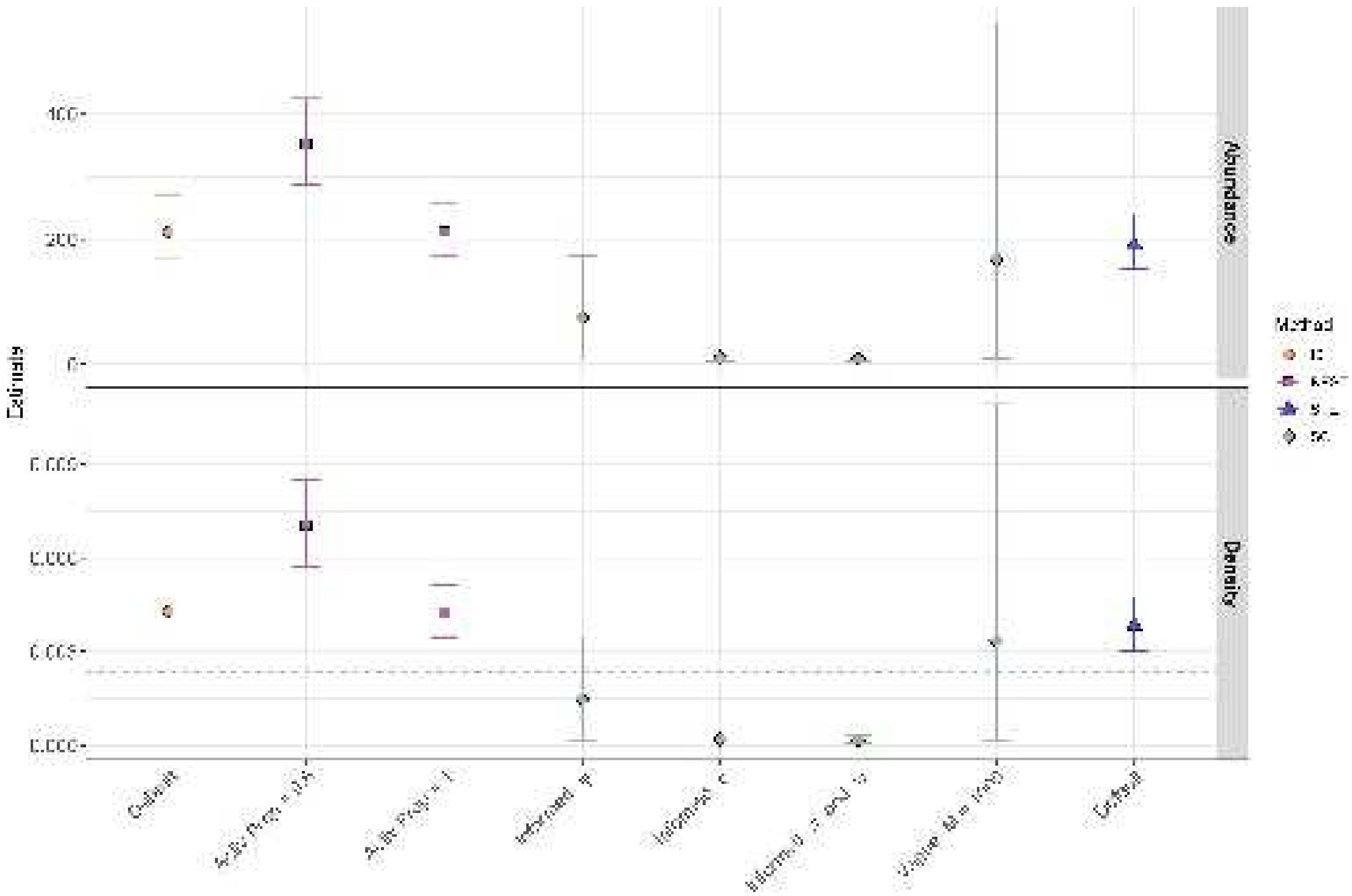

eap_2410_f3.png

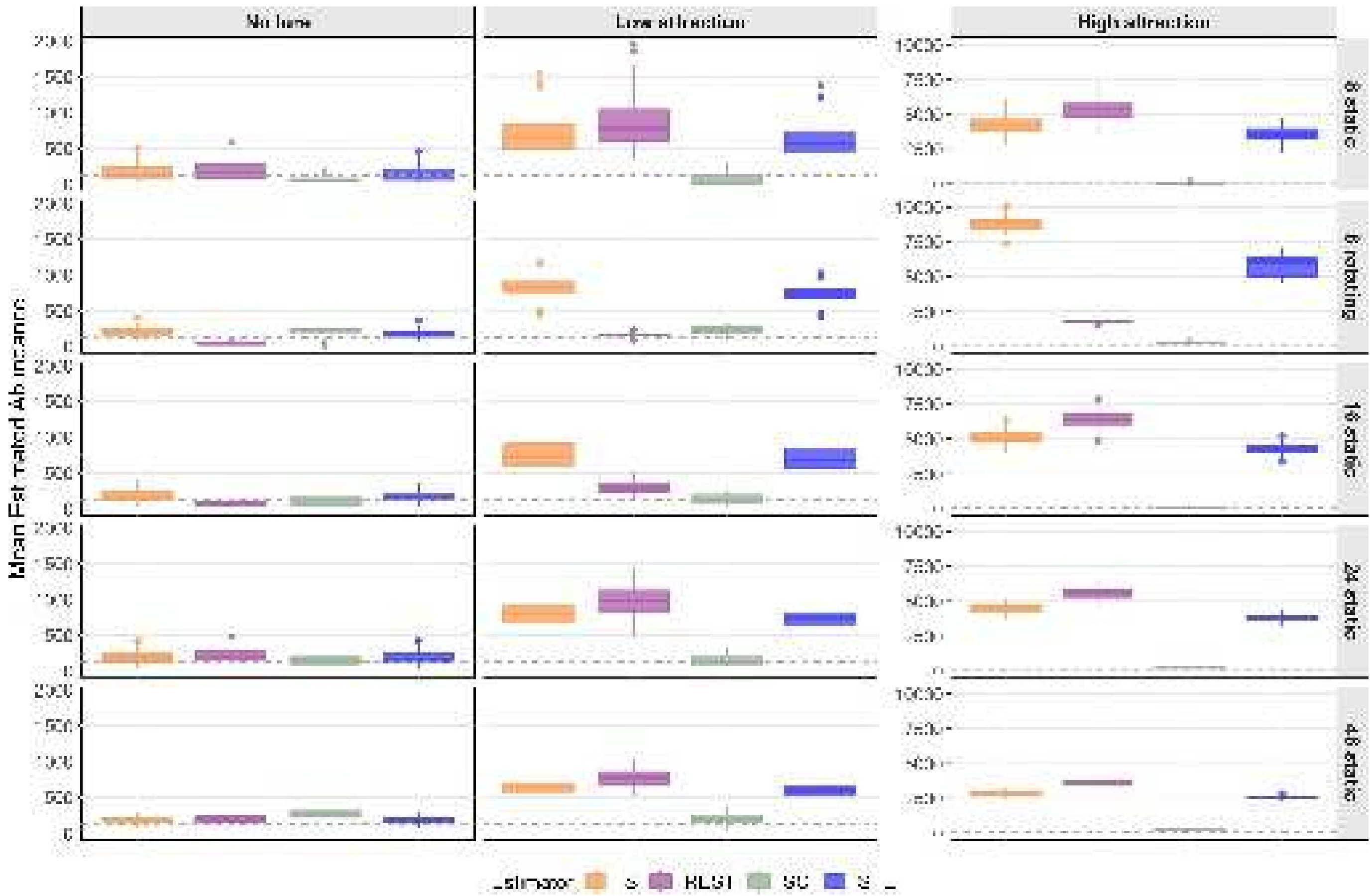

eap_2410_f4.png